A Multi Band Holey Based EBG Resonator Antenna for Performance Enhancement in UHF Band Frequency Range

[1]Gaurav Jain, [2]Nitesh Kumar
[1,2]Dept. of ECE, Sagar Institute of Research, Technology and Science, Bhopal, India

Abstract
A multi-frequency substrate integrated antenna with a large frequency difference is presented. It consists of a substrate-integrated Dielectric Resonator Antenna (DRA) for low- and high-frequency radiation, respectively. The structure is a using air holes and dual substrate. Beneath the antenna substrate is a second substrate. A Multi-frequency antenna working at S band, C band and X was designed, simulated, and measured. The S-parameters, VSWR, radiation patterns, excitation power, dispersive loss of material FR4 lossy are presented for different antenna structure and above parameters are reported. The results shows that Hole based MEBG antenna has main lobe magnitude between 14.9 dBv/m to 20 dBv/m with Angular Width (3dB) range from 27.4 to 47.1 degree and SLL of range -1.4 dB to -5.4 dB and having triple band of radiation with highest band width of 1.05 GHz for MEBG design with hole based structure. The minimum return loss is obtained for proposed design th is -24.37 dB at 6.44 GHz frequency the other bandwidth supported by the proposed design is 0.19 GHz and 0.33 GHz at 1.15 GHz and 4.53 GHz frequency. From the above research we can conclude that the presence of hole on EBG antenna leads towards multiband and modified ground plane with EBG structure improve the bandwidth of antenna along with higher magnitude of main lobe at radiating frequency range.

Keywords
Mushroom Electromagnetic Band Gap (MEBG), EBG Resonator Antenna (ERA), Broadband and Multi Band Shorting Pins

I. Introduction

ELECTROMAGNETIC band gap (EBG) structures have received tremendous amounts of attention in recent years [9]–[10]. The main advantages of these alternative structures include their ease and low cost of manufacture by virtue of hole techniques in printed-circuit technology, amenability to integration with planar circuits, high power-handling capacity, as well as lightweight nature, all these without compromising the overall essential properties of conventional antenna, which tend to be heavy, bulky, expensive to fabricate, and non integrable. Via-holes of circular cross section have been customary in the implementation of SIWs due to their ease and low cost of manufacture. However, in the advent of new fabrication techniques such as deep reactive-ion etching (DRIE), inductively coupled plasma etching (ICPE), and other modern laser technologies, via-holes of any shape can today be produced, e.g., [19]. A common EBG resonator antenna (ERA) consists of an air-filled half wavelength cavity formed between a perfect reflector (e.g., metallic ground plane or AMC) and a high-reflectivity top. This top section can take various forms, depending upon the design methodology and fabrication technology, including 3-D EBG structures, in this paper we are using 2-D printed frequency-selective surfaces and stacks of unprinted dielectric slabs [4-5] along with the hole array on the proposed structure. Here, we use the general term superstructure to refer to all such top sections. A variety of antenna design has been investigated. Their size reduction [6], [11]; bandwidth enhancement [11]–[16] and making them workable for multi band range, have been addressed for applications, such as cell phone, global satellite coverage, feed clusters for multiple-beam antennas in space applications, and point-to-point microwave links in frequency range of 1 to 8 GHz.

In this paper we present different EBG-via-hole structure in which single dielectric substrate material of FR4 is used. By applying the superstrate to the microstrip antenna, a wider application such as radome and housing can be possible. To create an in-phase radiation aperture, the effective permittivity of the superstrate at each position is controlled by drilling holes in the dielectric layer. In section II, prologue to the theory and formulation of superstrate is studied. In section III, Antenna configuration is presented. In section IV, results of various cases are compared. And finally, a conclusion is reached in section V.

II. Prologue to the Theory and Formulation

The electric field distribution of the antenna aperture and the radiation pattern have a Fourier transform relationship. Therefore in order to create a high gain antenna, it is not only necessary to have a larger antenna aperture, but there should also be an in-phase electric field on the aperture [1]. Let us assume a point source as shown in fig. 1. The phase of the electric field some distance away from the point source is dependent on the distance. The phase difference ($\Delta\xi$) between observations points P1and P2 in the air can be expressed as following equation.

$$2n\pi + \Delta\xi = \beta_0(\sqrt{d^2 + l^2} - d) \qquad (1)$$

Where β_0 is the propagation constant in the air, d is the distance between the point source and P1, l is the distance between P1and P2. According to (1), the phase difference is always nonzero when the distance l is not zero. When a dielectric layer which has a thickness of d2 with a different permittivity determined by its position is located above the point source at a distance of d1, the phase difference ($\Delta\xi$) between points P1and P2 can be expressed by the following equation, assuming that there is no reflection between the dielectric layer and the air:

$$2n\pi + \Delta\xi = \beta_0(\sqrt{d^2 + l^2} - d_1) + d_2\beta_0(\sqrt{\varepsilon_1} - \sqrt{\varepsilon_2}) \qquad (2)$$

Where ε_2 is the permittivity at P2 and ε_1 is permittivity at P1. According to (2) the phase difference $\Delta\xi$ can be set to zero by ε_2.

The effective permittivity can be controlled by changing the properties of the material, such as its thickness. The air holes are characterized by their separations s_a and diameter d_a. The metallic posts are characterized by their separations s_v and diameter d_v. Their values must be appropriately chosen [Deslandes and Wu,

2001] in order to avoid radiation losses, so they must fulfill the following conditions:

$$d_v < \lambda g/5, \quad s_v \leq 2dv \tag{3}$$

where λg is the guided wavelength. In this paper, creating holes in the dielectric layer is suggested in order to obtain different effective permittivities according to the size of the holes. the effective ε_{reff} obtained after making the air holes in the propagation area in order to reduce the antenna effective permittivity. Moreover, a decrease of the dielectric losses is expected due to the removal of material. The effective permittivity is given by the following equation:

$$\varepsilon_{reff} = \frac{c^2}{4a_{eff}^2 f_c^2} \tag{4}$$

Where c is the speed of light in free space is the effective width of structure and is the cutoff frequency. CST MWS, a 3D FDTD based EM simulation, was used to choose the proper hole size. Fig. 2(a) shows a unit cell simulation structure. PEC and PMC boundary conditions are used. Since multiple reflections occur at the surface of the dielectric layer it was possible to obtain the relationship between hole size and effective permittivity using a unit cell simulation.

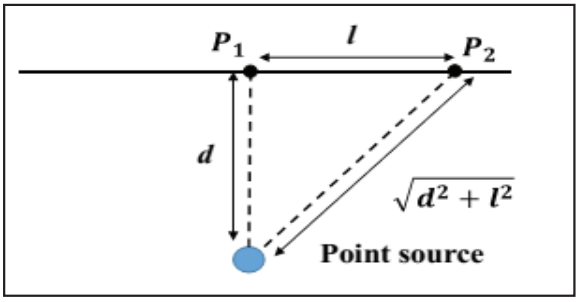

(a)

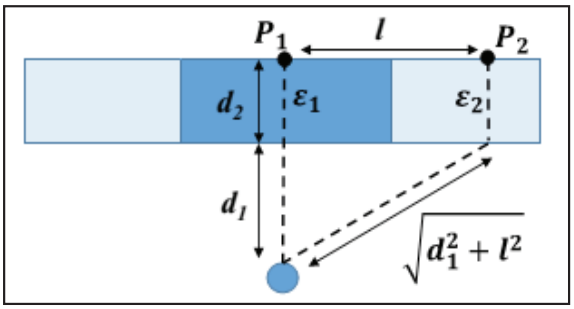

(b)

Fig. 1: Phase Difference Between Two Points for the Air (a) and Effective Superstrate (b)

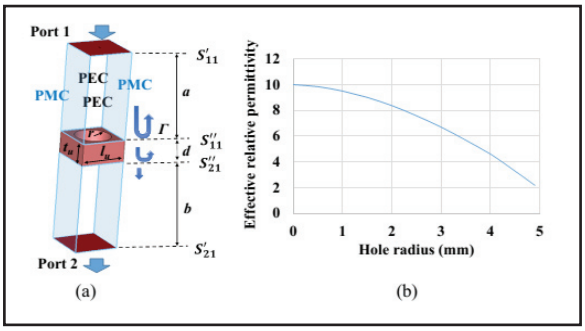

(a) (b)

Fig. 2: Unit Cell Simulation Model (a) and Extracted Effective Permittivity for the Different Hole Radius (b)

It is observed that the value of the effective permittivity is inversely proportional to the radius of the holes [1]. With respect to holes with a radius of 1, 2, 3, and 4 mm, the values of effective permittivity are calculated as 9.5, 8.3, 6.5, and 4.5. The top and bottom dual-metal-plane conductors are connected by the periodically metallic via-hole within the designed substrate. With the appropriate height of substrate and separation between the adjacent metallic via-holes, an excellent parallel-plate-metal synthesised transmission line with an improved coupling between the top and bottom resonators can be achieved by this via-hole-loaded technology. The metallic circular holes are designed as both phase shifters and radiating elements, which are feed by coaxial feed.

III. Antenna Configuration

The configuration of different antennas are presented which has different bands of operation shown in fig. 3. Its design has been inspired by Mushroom type EBG (MEBG) patch antenna with [1], [3], [5], [25], and its radiation mechanism can be described in terms of defect modes as in [1], [3], and [25] or using the cavity resonance condition [2]. Its superstructure consists of two identical printed dielectric slabs placed back to back with a thickness of 4 mm each, which has mushroom type EBG structure on top of the upper substrate material and PEC at the bottom of second structure, of dimension of (80 × 80) mm². The two substrates are 4 mm thick FR 4 lossy material with ε_r=4.3. We have presented 4 design of antenna in the paper each having similar substrate structure and dimension but the effect of hole and shorting pins with some parasitic patch on the top of the second substrate and modified ground plane is presented in different design.

A. Mushroom EBG Design With Shorting Pins

The antenna design consists of two double sided printed PCB with dielectric material as FR4 of dimensions (80 × 80) mm² with thickness of 4 mm each shown in fig. 3. In this structure we use shorting pins of radius 2 mm and height of 8 mm PEC material crossing both substrate, and the ground plane of both substrate is PEC material of dimension (80 × 80) mm² each.

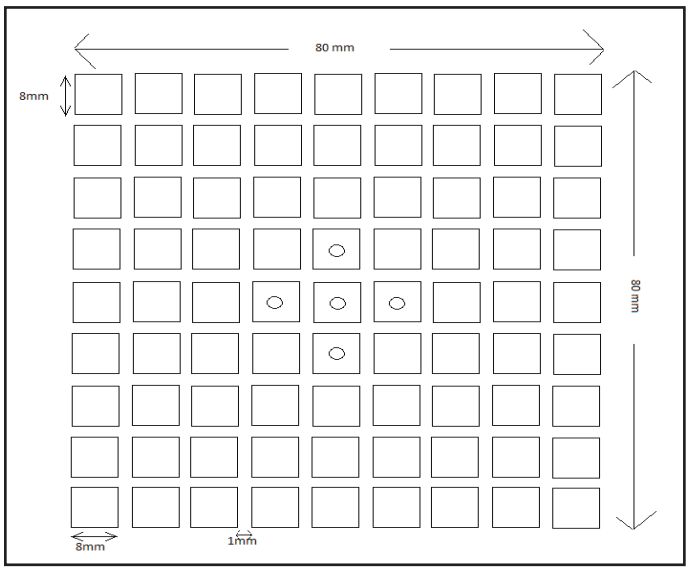

Fig. 3: Top View of the 1st Substrate Printed Mushroom EBG (MEBG) Structure

The each cell of MEBG structure has a dimension (8× 8) mm², and the unprinted gap of 1 mm between each cell shown in fig. 3. The bottom of 1st substrate, top of 2nd substrate and bottom of 2nd substrate is shown in Fig. 4, Fig. 5, and Fig. 6 respectively.

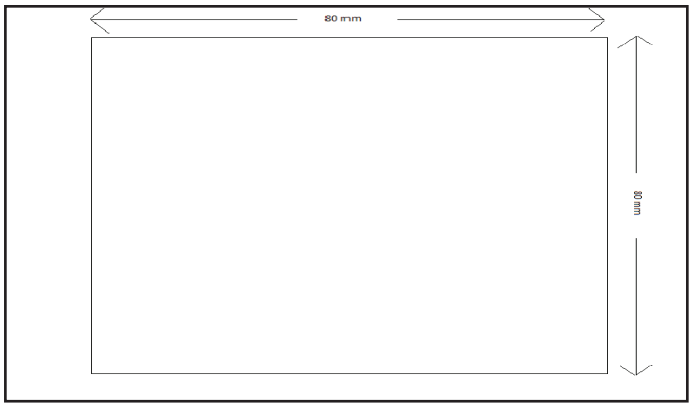

Fig. 4: Bottom View of the 1st Substrate Printed Mushroom EBG (MEBG) Structure.

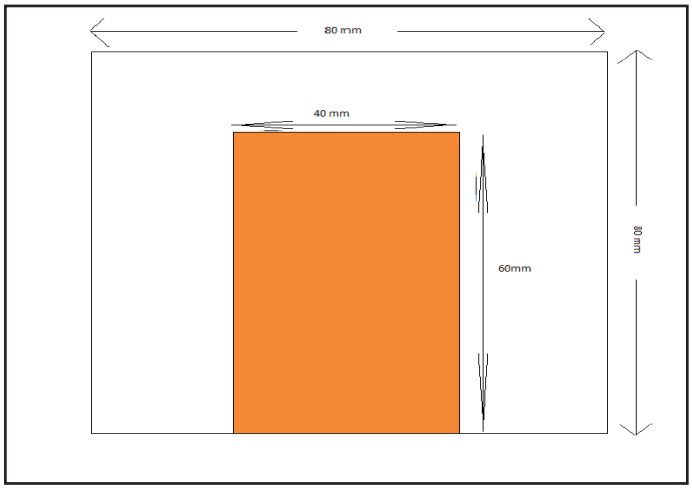

Fig. 5: Top View of the 2nd Substrate Printed Mushroom EBG (MEBG) Structure.

The top of 2nd substrate has a metallic patch of dimensions of (30× 60) mm² and the ground plain which is bottom of 2nd substrate has two metallic patches of dimensions (8× 80) mm² each shown in fig. 6.

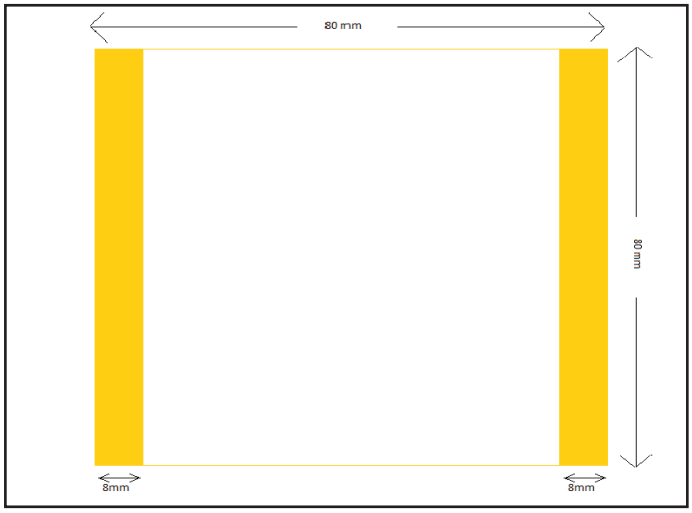

Fig. 6. Bottom view of the 2nd substrate printed Mushroom EBG (MEBG) structure.

B. Mushroom EBG Design with Shorting Pins and one Hole at Center

The design of the antenna is almost same as that of previous design the only difference in top of 1st substrate is that, we introduced one hole of radius 2mm and two more shorting pins are introduced on opposite coordinates shown in Fig. 7 and top of 2nd substrate patch is modified with the dimensions of (50× 40) mm² shown in Fig. 9 rest of the design is same as that of previous design.

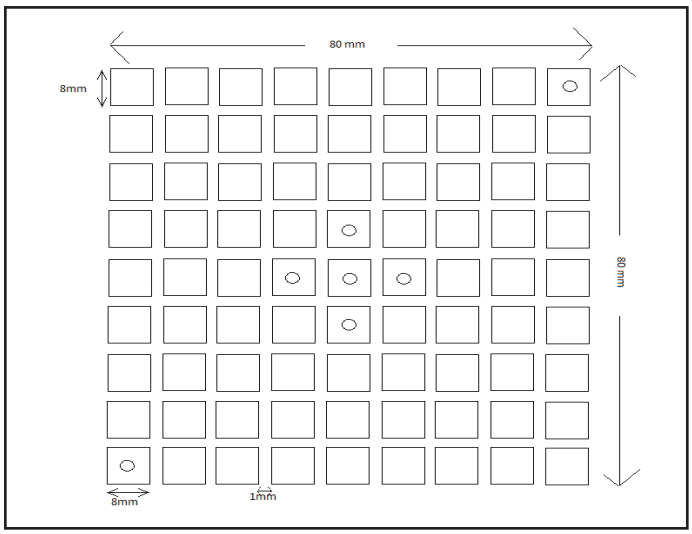

Fig. 7: Top View of the 1st Substrate Printed Mushroom EBG (MEBG) Structure With One Hole at Center.

Fig. 8: Bottom View of the 1st Substrate Printed Mushroom EBG (MEBG) Structure

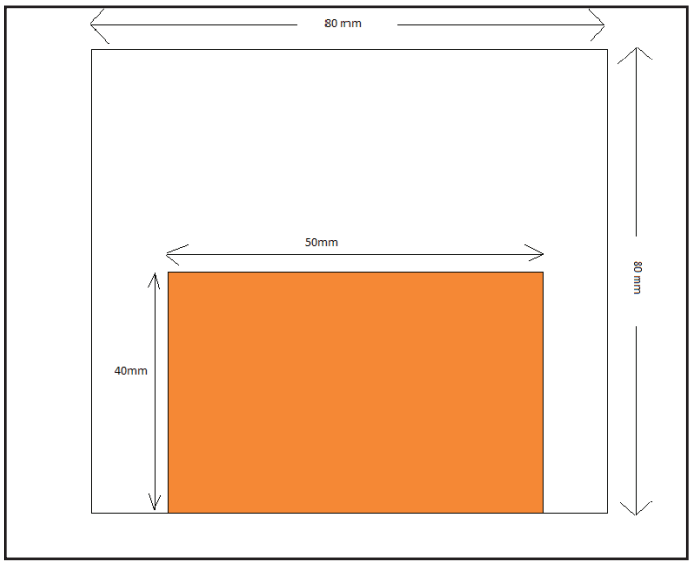

Fig. 9: Top View of the 2nd Substrate Printed Mushroom EBG (MEBG) Structure

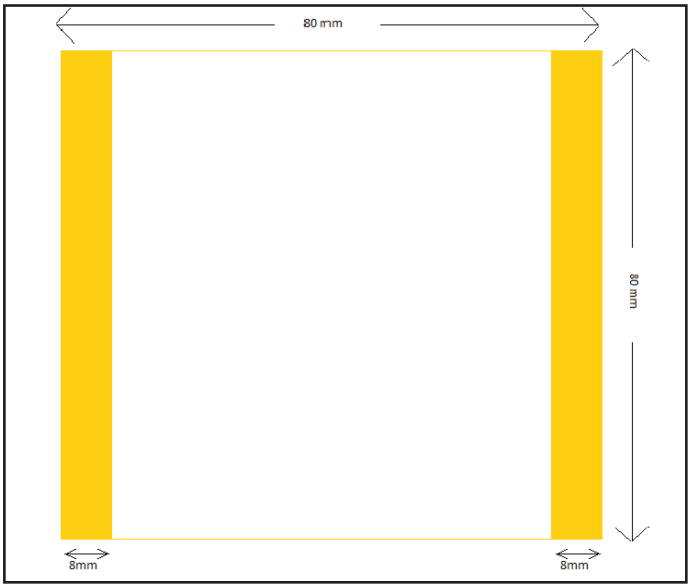

Fig. 10: Bottom View of the 2nd Substrate Printed Mushroom EBG (MEBG) Structure

C. Mushroom EBG Design with Shorting Pins and One Hole at Center with Modified Patch of 2nd Substrate

The design of the antenna is almost same as that of design B. the only difference in the top of 2nd substrate patch which is modified with two metallic patch with the dimensions of (6030) and (6010) with a gap of 20 mm shown in fig. 13. rest of the design is same as that of previous design.

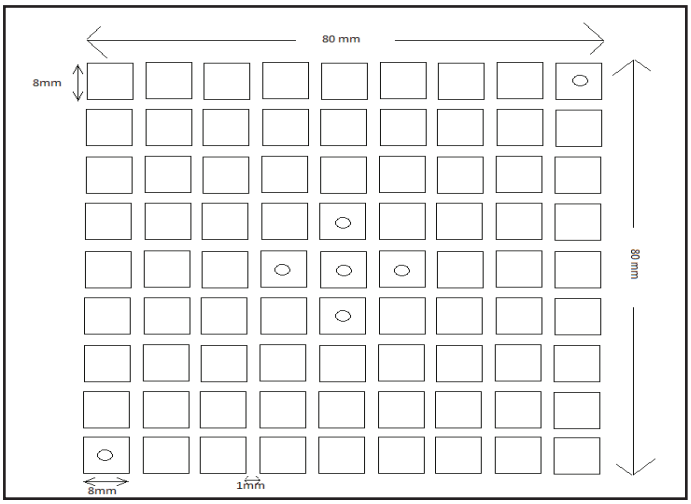

Fig. 11: Top View of the 1st Substrate Printed Mushroom EBG (MEBG) structure with one hole at center.

Fig. 12: Bottom View of the 1st Substrate Printed Mushroom EBG (MEBG) Structure.

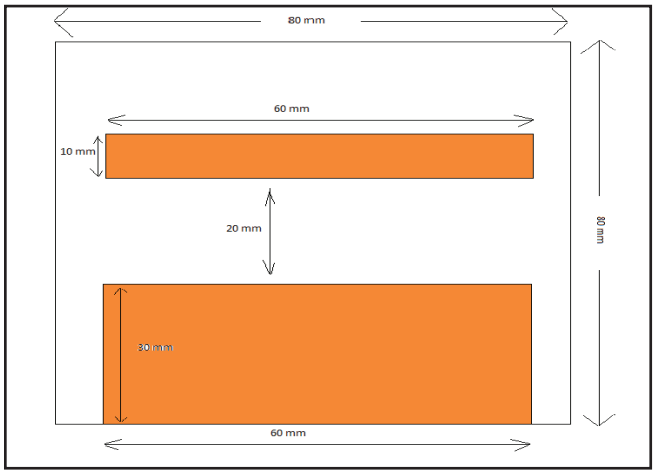

Fig. 13: Top View of the 2nd Substrate Printed Mushroom EBG (MEBG) Structure

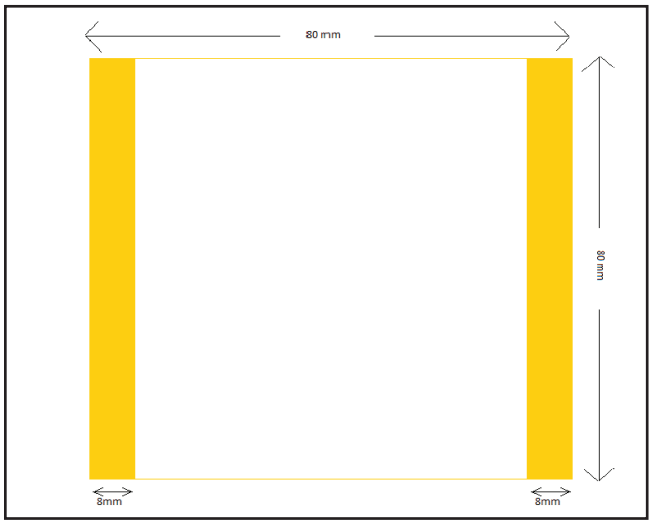

Fig. 14: Bottom view of the 2nd substrate printed Mushroom EBG (MEBG) structure.

D. Mushroom EBG Design With Holes and Modified Patch of 2nd Substrate

The design of the antenna is almost same as that of design B. the only difference is that we introduced holes on the top of mushroom EBG structure in place of shorting pins, the radius of each holes are 2 mm shown in Fig.15. rest of the design is same as that of design B.

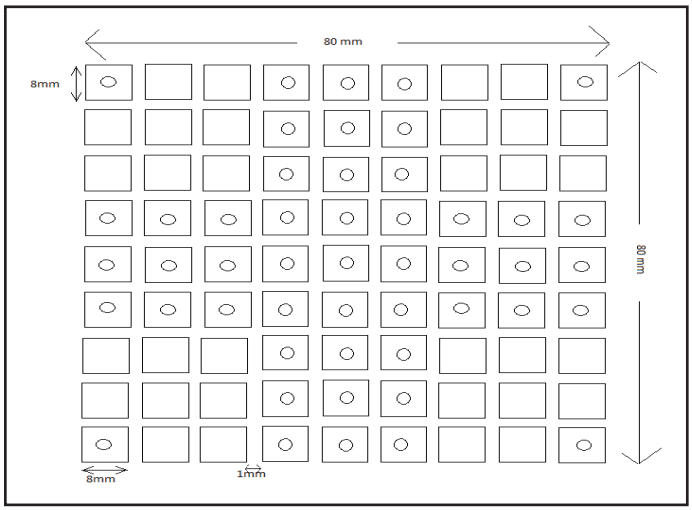

Fig. 15: Top View of the 1st Substrate Printed Mushroom EBG (MEBG) Structure With One Hole at Center.

Fig. 16: Bottom view of the 1st Substrate Printed Mushroom EBG (MEBG) structure.

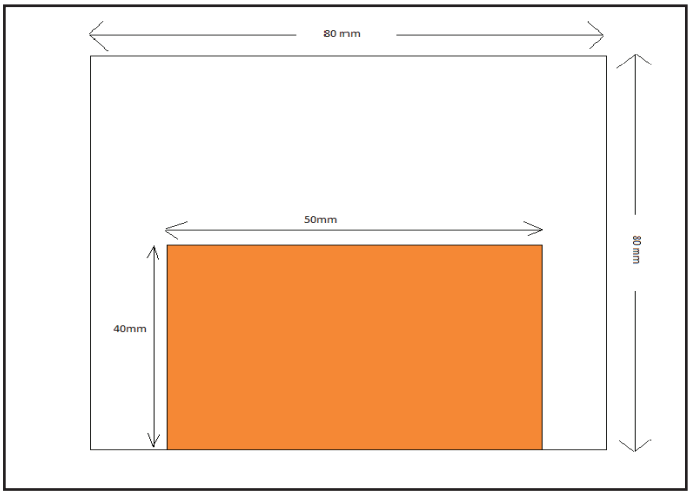

Fig.17. Top view of the 2nd Substrate Printed Mushroom EBG (MEBG) Structure.

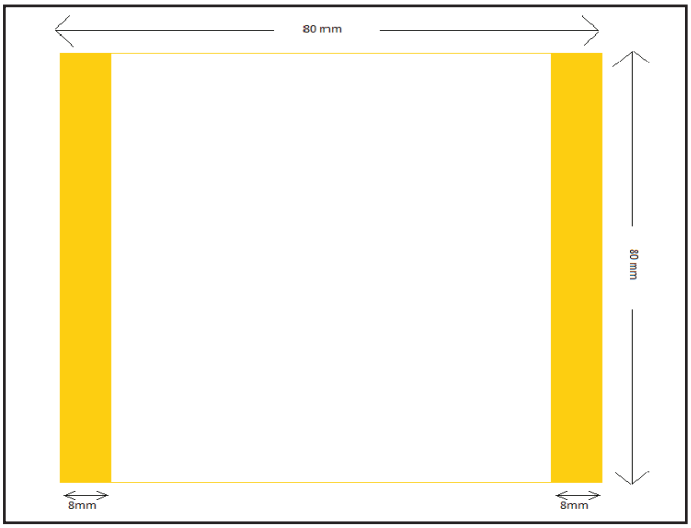

Fig.18. Bottom view of the 2nd substrate printed Mushroom EBG (MEBG) structure.

IV. Simulation Results

The simulation result carried out on CST Microwave studio suite for the different MEBG antenna with shorting pins, holes and modified printed structure of 2nd substrate. The S_{11} for the above designs are presented in fig. 19 and summarized in the Table 1.

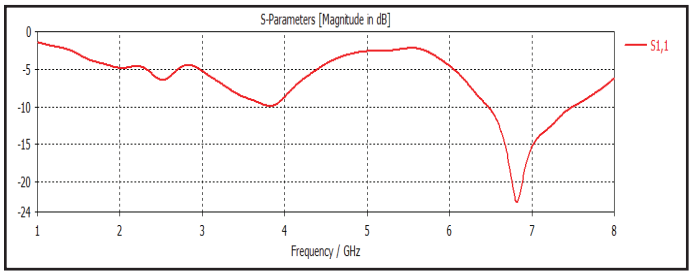

Fig. 19: S_{11} For Design (A) of printed Mushroom EBG (MEBG) Structure With Shorting Pins.

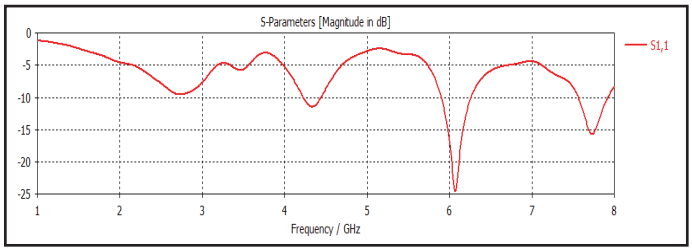

Fig. 20: S_{11} For Design (B) of Printed Mushroom EBG (MEBG) Structure

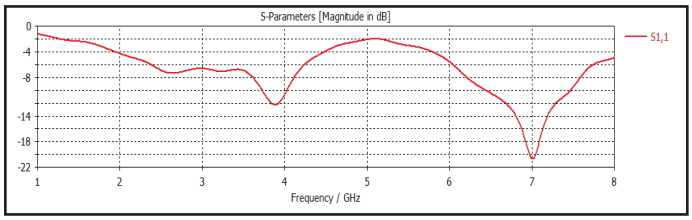

Fig. 21: S_{11} For Design (C) of Printed Mushroom EBG (MEBG) Structure

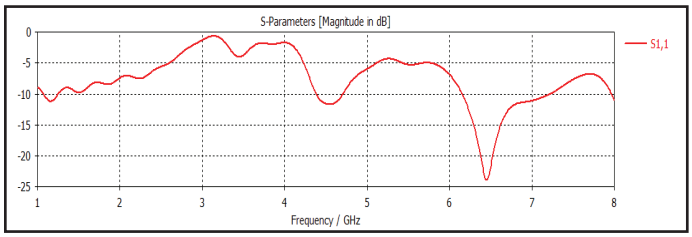

Fig. 22: S_{11} For Design (D) of Printed Mushroom EBG (MEBG) Structure

Table 1: Of Simulation Result Of Proposed Design

Design	Minimum return loss (dB)	Bandwidth (GHz)	Minimum VSWR at radiating frequency	Electric Dispersion at radiating frequency	Number of operating band
A	-22.815 at 6.82 GHz	1.04	1.1 at 6.82 GHz	0.1 at 6.82 GHz	Single
B	-11.516 (4.33 GHz)	0.22	1.07 at 6.07 GHz	0.104 (4.33 GHz)	Triple
	-24.72 (6.07 GHz)	0.36		0.108 (6.07 GHz)	
	-15.78 (7.73 GHz)	0.36		0.194 (7.73 GHz)	
C	-12.27 (3.87 GHz)	0.30	1.03 at 7.00 GHz	0.103 (3.87 GHz)	Double
	-20.75 (7.00 GHz)	1.04		0.109 (7.00 GHz)	
D	-11.29 (1.15 GHz)	0.19	1.05 at 6.44 GHz	0.109 (1.15 GHz)	Triple
	-11.96 (4.53 GHz)	0.33		0.105 (4.53 GHz)	
	-24.21 (6.44 GHz)	1.05		0.108 (6.44 GHz)	

The electric dispersion of the dielectric material FR4 with respect to operating frequency is shown in fig. 23 and the far field pattern of all proposed design is shown in fig. 24, fig. 25 and fig. 26 for the different frequency, detail of far field result is tabulated in Table 2 with main lobe magnitude, angular width (3 dB) and Side Lobe Level (SSL).

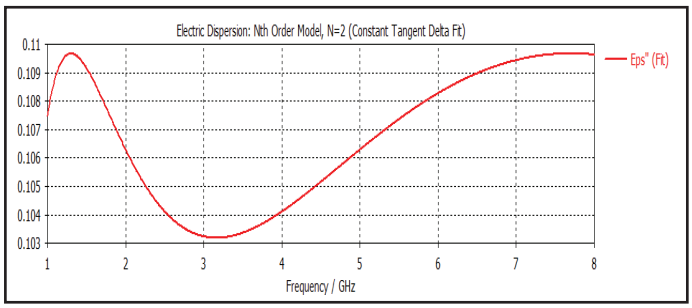

Fig. 23: Electric Dispersion of the Dielectric Material FR4 with Respect to Frequency

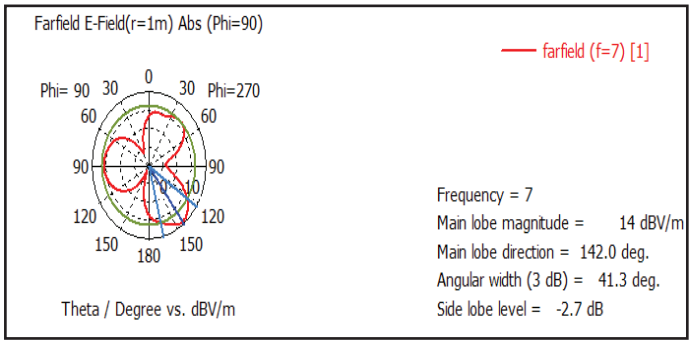

Fig. 24: Far Field Pattern for Design (A) at Frequency 7 GHz.

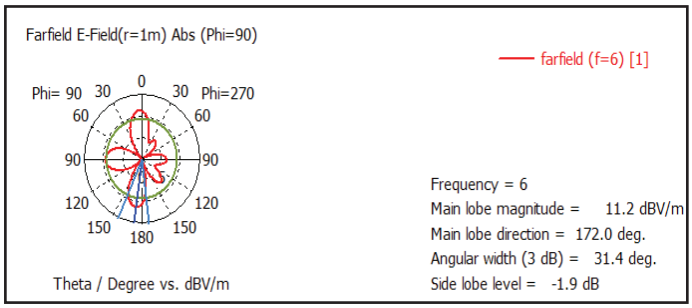

Fig. 25: Far Field Pattern for Design (B) at Frequency 6 GHz.

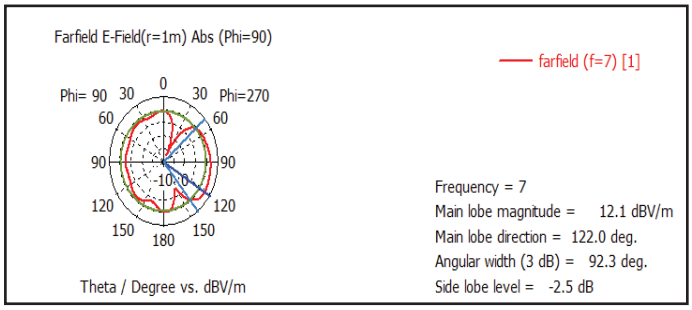

Fig. 26: Far Field Pattern for Design (C) at Frequency 7 GHz.

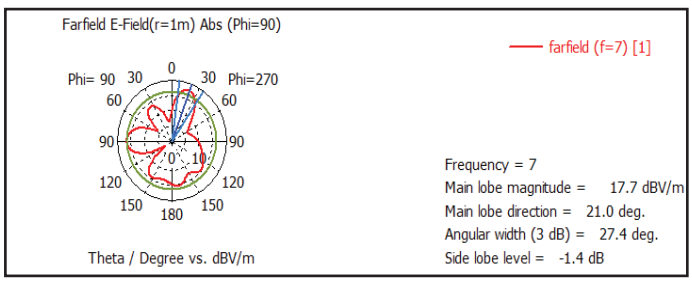

Fig. 26: Far Field Pattern for Design (D) at Frequency 7 GHz.

Table 2: Far Field Pattern for Design A.

Frequency (GHz)	Main Lobe Magnitude (dBV/m)	Angular Width (3dB) in degree	Side Lobe Level (SLL) (dB)
2	0.38	347°	Not present
3	8.96	220°	Not present
4	10.90	62.6°	Not present
5	10.10	60.2°	-2.9
6	12.90	34.9°	-2.8
7	14.00	41.3°	-2.7
8	11.50	40.0°	-2.0

Table 3: Far Field Pattern For Design B.

Frequency (GHz)	Main Lobe Magnitude (dBV/m)	Angular Width (3dB) in degree	Side Lobe Level (SLL) (dB)
2	-0.98	57.4°	-3
3	5.47	45.4°	-4.7
4	9.38	45.1°	-1.6
5	9.59	47.1°	-2.0
6	11.20	31.4°	-1.9
7	12.70	26.0°	-1.8
8	13.70	31.5°	-2.9

Table 4: Far Field Pattern For Design C.

Frequency (GHz)	Main Lobe Magnitude (dBV/m)	Angular Width (3dB) in degree	Side Lobe Level (SLL) (dB)
2	-0.02	197.8°	Not present
3	8.61	68.9°	-1.9
4	10.20	41.2°	-4.9
5	9.75	44.3°	-0.9
6	11.60	79.6°	-1.2
7	12.10	92.3°	-2.5
8	9.95	25.6°	-4.0

Table 5: Far Field Pattern for Design D.

Frequency (GHz)	Main Lobe Magnitude (dBV/m)	Angular Width (3dB) in degree	Side Lobe Level (SLL) (dB)
2	10.30	54.6°	-1.8
3	14.90	47.1°	-5.4
4	-6.25	48.8°	-3.1
5	14.50	38.0°	-2.1
6	16.70	29.2°	-3.0
7	17.70	27.4°	-1.4
8	20.00	23.6°	-1.5

The simulated radiation patterns of all the design with shorting pins and hole based MEBG antenna at different frequency is tabulated in Table II, III, IV and V from which we know that the maximum gain is achieved for design D which is a hole based Mushroom EBG antenna at the frequency at 6 to 8 GHz.

V. Conclusion

Out of four design presented above so far is multi band structure is considered design B, C and design D are having triple, double and triple band respectively with highest band width of 1.05 GHz for design D with hole based structure. The minimum return loss is obtained for design D that is -24.37 dB at 6.44 GHz frequency the other bandwidth supported by the design D is 0.19 GHz and 0.33 GHz at 1.15 GHz and 4.53 GHz frequency. From the above research we can conclude that the presence of hole on EBG antenna leads it towards multiband and modified ground plane with EBG

structure improve the bandwidth of antenna along with higher magnitude of main lobe at radiating frequency range. Hole based MEBG antenna has main lobe magnitude between 14.9 dBv/m to 20 dBv/m with Angular Width (3dB) range from 27.4 to 47.1 degree and SLL of range -1.4 dB to -5.4 dB.

References

[1] Jae Hee Kim, Chi-Hyung Ahn, Jin-Kyu Bang,"Antenna Gain Enhancement using a Holey Superstrate", IEEE Transactions On Antennas And Propagation, Vol. 64, No. 3, March 2016.

[2] Xiaoyan Zhang, Zhaopeng Teng, Zhiqing Liu, Bincheng Li.,"A Dual Band Patch Antenna with a Pinwheel-Shaped Slots EBG Substrate", Hindawi Publishing Corporation International Journal of Antennas and Propagation Volume 2015, Article ID 815751.

[3] Raheel M. Hashmi, Basit A. Zeb.,"Wideband High-Gain EBG Resonator Antennas with Small Footprints and All-Dielectric Superstructures", IEEE Transactions On Antennas And Propagation, Vol. 62, No. 6, June 2014.

[4] Osama M. Haraz,"Dense Dielectric Patch Array Antenna With Improved Radiation Characteristics Using EBG Ground Structure and Dielectric Superstrate for Future 5G Cellular Networks", IEEE. Translations Vol. 2, 2014.

[5] Weiwei Xu, Junhong Wang,"A Novel Microstrip Antenna With Composite Patch Structure for Reduction of In-Band RCS". IEEE Antennas And Wireless Propagation Letters, Vol. 14, 2015.

[6] Basit Ali Zeb Nasiha Nikolic, Karu P. Esselle,"A High-Gain Dual Band EBG Resonator Antenna with Circular Polarization IEEE Antennas And Wireless Propagation Letters", Vol. 14, 2015.

[7] Jae-Yeong Lee, Seung-Han Kim, Jae-Hyung Jang, "Reduction of Mutual Coupling in Planar Multiple Antenna by Using 1-D EBG and SRR Structures", IEEE Transactions On Antennas and Propagation, Vol. 63, No. 9, September 2015.

[8] Changrong Liu,"Capacitively Loaded Circularly Polarized Implantable Patch Antenna for ISM Band Biomedical Applications", IEEE Transactions On Antennas And Propagation, Vol. 62, No. 5, May 2014.

[9] Quan Wei Lin, Hang Wong,"Printed Meandering Probe-Fed Circularly Polarized Patch Antenna With Wide Bandwidth IEEE Antennas And Wireless Propagation Letters, Vol. 13, 2014.

[10] Chao Sun, Huili Zheng, Lingfei Zhang, Ying Liu, "Analysis and Design of a Novel Coupled Shorting Strip for Compact Patch Antenna with Bandwidth Enhancement", IEEE Antennas And Wireless Propagation Letters, Vol. 13, 2014.

[11] Md. Shahidul Alam,"Development of Electromagnetic Band Gap Structures in the Perspective of Microstrip Antenna Design", Hindawi Publishing Corporation International Journal of Antennas and Propagation, Vol. 2013, Article ID 507158.

[12] Constantine A. Balanis,"Antenna Theory, Analysis and Design", John Wiley & Sons Inc. 3rd edition. 2005.

[13] K. Buell, H. Mosallaei, K. Sarabandi,"Metamaterial insulator enabled super directive array," IEEE Trans. Antennas Propag., Vol. 55, No. 4, pp. 1074–1085, Apr. 2007.

[14] Ramesh Garg, Apisak Ittipiboon,"Microsrtip Antenna Design Hand Book", Artech House, Inc. 2001.

[15] M. M. Bait-Suwailam, O. F. Siddiqui, O. M. Ramahi, "Mutual Coupling Reduction Between Microstrip Patch Antennas Using Slotted-Complementary SplitRing Resonators", IEEE Antennas and Wireless Propagation Letters, Vol. 9, pp. 876-878, 2010.

[16] Y. Lee, J. Yeo, R. Mittra,"Investigation of electromagnetic band gap (EBG) structures for antenna pattern control", In Proceedings of the IEEE International Antennas and Propagation Symposium, Vol. 2, pp. 1115–1118, June 2003.

[17] Y. Horii, M. Tsutsumi,"Wide band operation of a harmonically controlled EBG microstrip patch antenna", In Proceedings of the IEEE Antennas and Propagation Society International Symposium, Vol. 3, pp. 768–771, San Antonio, Tex, USA, June 2002.

[18] J. Y. Lee, S. H. Kim, J. H. Jang,"Reduction of Mutual Coupling in Planar Multiple Antenna by Using 1-D EBG and SRR Structures" IEEE Trans. Antennas and Propagation, Vol. 63, No. 9, pp. 4194-4198, Sept. 2015.

[19] C. Cheype, C. Serier, M. Thevenot, T. Monediere, A. Reineix, B.Jecko,"An electromagnetic bandgap resonator antenna," IEEE Trans. Antennas Propag., Vol. 50, No. 9, pp. 1285–1290, Sep. 2002.

[20] Naizhi Wang, Qiang Liu.,"Wideband Fabry-Perot Resonator Antenna With Two Complementary FSS Layers". IEEE Transactions on Antennas and Propagation, Vol. 62, No. 5, May 2014.